Inorg. Chem. **2007**, *46*, 10208–10213

Porous Metal–Organic Frameworks Based on Metal–Organic Polyhedra with Nanosized Cavities as Supramolecular Building Blocks: Two-Fold Interpenetrating Primitive Cubic Networks of $[Cu_6L_8]^{12+}$ Nanocages

Jaejoon Park,[†] Seunghee Hong,[†] Dohyun Moon,[†] Mira Park,[†] Kyungjin Lee,[†] Sangmi Kang,[†] Yang Zou,[†] Rohith P. John,[†] Ghyung Hwa Kim,[‡] and Myoung Soo Lah*,[†]

Department of Chemistry and Applied Chemistry, College of Science and Technology, Hanyang University, Ansan, Kyunggi-Do 426-791, Korea and Pohang Accelerator Laboratory, Pohang, Kyungbook 790-784, Korea

Received July 10, 2007

Discrete metal–organic polyhedra (MOP) with nanosized cavities and/or clusters of MOP could be prepared when C_3-symmetric facial ligands and a potential hexatopic Cu(II) ion are combined in the presence of perchlorate as a weak linker, while similar reaction conditions in the presence of a nitrate linker led to extended metal–organic frameworks made of MOP as supramolecular building blocks.

Introduction

Construction of porous metal−organic frameworks (MOFs) is an attractive aim because of their potential applications in storage,[1] separation,[2] and catalysis.[3] The appropriate design of ligands and metal building units has led to various interesting porous MOFs.[4] However, control of the shape and properties of the cavity formed is still challenging. Small changes in the building unit can lead to a completely different framework topology rather than an isostructural network with tuned cavity shape and properties. The strategy that uses secondary building units (SBUs) has provided a better approach for the construction of nanoporous isostructural MOFs with some specific network topologies.[5] Another way for the construction of nanoporous MOFs is the use of supramolecular building blocks (SBBs).[6] When highly symmetric metal−organic polyhedra (MOP) with nanosized cavities are used as SBBs, the resulting frameworks will have nanosized cavities regardless of the network topology. Utilization of MOP with nanosized cavities as the building blocks for the MOFs can guarantee the generation of a porous framework because the building block itself has a cavity and the interpenetration does not affect the cavity of the building blocks. In addition, properties such as the shape and functionality of the cavity can be controlled or tuned at the

* To whom correspondence should be addressed. Phone: 82 31 400 5496. Fax: 82 31 436 8100. E-mail: mslah@hanyang.ac.kr.
[†] Hanyang University.
[‡] Pohang Accelerator Laboratory.

(1) (a) Rowsell, J. L. C.; Yaghi, O. M. *Angew. Chem., Int. Ed.* **2005**, *44*, 4670. (b) Rowsell, J. L. C.; Spencer, E. C.; Eckert, J.; Howard, J. A. K.; Yaghi, O. M. *Science* **2005**, *309*, 1350. (c) Rosi, N. L.; Eckert, J.; Eddaoudi, M.; Vodak, D. T.; Kim, J.; O'Keeffe, M.; Yaghi, O. M. *Science* **2003**, *300*, 1127. (d) Zhao, X.; Xiao, B.; Fletcher, A. J.; Thomas, K. M.; Bradshaw, D.; Rosseinsky, M. J. *Science* **2004**, *306*, 1012.

(2) (a) Kuznicki, S. M.; Bell, V. A.; Nair, S.; Hillhouse, H. W.; Jacubinas, R. M.; Braunbarth, C. M.; Toby, B. H.; Tsapatsis, M. *Nature* **2001**, *412*, 720. (b) Kosal, M. E.; Chou, J.-H.; Wilson, S. R.; Suslick, K. S. *Nat. Mater.* **2002**, *1*, 118. (c) Bradshaw, D.; Prior, T. J.; Cussen, E. J.; Claridge, J. B.; Rosseinsky, M. J. *J. Am. Chem. Soc.* **2004**, *126*, 6106. (d) Jiang, C.; Lesbani, A.; Kawamoto, R.; Uchida, S.; Mizuno, N. *J. Am. Chem. Soc.* **2006**, *128*, 14240. (e) Chen, B.; Liang, C.; Yang, J.; Contreras, D. S.; Clancy, Y. L.; Lobkovsky, E. B.; Yaghi, O. M.; Dai, S. *Angew. Chem., Int. Ed.* **2006**, *45*, 1390.

(3) (a) Ohmori, O.; Fujita, M. *Chem. Commun.* **2004**, 1586. (b) Seo, J. S.; Whang, D.; Lee, H.; Jun, S. I.; Oh, J.; Jeon, Y. J.; Kim, K. *Nature* **2000**, *404*, 982. (c) Uemura, T.; Kitaura, R.; Ohta, Y.; Nagaoka, M.; Kitagawa, S. *Angew. Chem., Int. Ed.* **2006**, *45*, 4112. (d) Zou, R.-Q.; Sakurai, H.; Xu, Q. *Angew. Chem., Int. Ed.* **2006**, *45*, 2542. (e) Wu, C.-D.; Hu, A.; Zhang, L.; Lin, W. *J. Am. Chem. Soc.* **2005**, *127*, 8940.

(4) (a) Ockwig, N. W.; Delgado-Friedrichs, O.; O'Keeffe, M.; Yaghi, O. M. *Acc. Chem. Res.* **2005**, *38*, 176. (b) Mellot-Draznieks, C.; Dutour, J.; Ferey, G. *Angew. Chem., Int. Ed.* **2004**, *43*, 6290. (c) Eddaoudi, M.; Kim, J.; Rosi, N.; Vodak, D.; Wachter, J.; O'Keeffe, M.; Yaghi, O. M. *Science* **2002**, *295*, 469. (d) Kitagawa, S.; Kitaura, R.; Noro, S. *Angew. Chem., Int. Ed.* **2004**, *43*, 2334. (e) Moulton, B.; Zaworotko, M. J. *Chem. Rev.* **2001**, *101*, 1629.

(5) (a) Eddaoudi, M.; Moler, D. B.; Li, H.; Chen, B.; Reineke, T. M.; Keeffe, M. O.; Yaghi, O. M. *Acc. Chem. Res.* **2001**, *34*, 319. (b) Cotton, F. A.; Lin, C.; Murillo, C. A. *Acc. Chem. Res.* **2001**, *34*, 759. (c) Yaghi, O. M.; O'Keeffe, M.; Ockwig, N. W.; Chae, H. K.; Eddaoudi, M.; Kim, J. *Nature* **2003**, *423*, 705. (d) Chae, H. K.; Siberio-Pérez, D. Y.; Kim, J.; Go, Y.; Eddaudi, M.; Matzger, A.; O'Keeffe, M.; Yaghi, O. M. *Nature* **2004**, *427*, 523. (e) Li, H.; Laine, A.; O' Keeffe, M.; Yaghi, O. M. *Science* **1999**, *283*, 1145.

(6) (a) O'Keeffe, M.; Eddaoudi, M.; Li, H. L.; Reineke, T.; Yaghi, O. M. *J. Solid State Chem.* **2000**, *152*, 3. (b) Lee, E.; Kim, J.; Heo, J.; Whang, D.; Kim, K. *Angew. Chem., Int. Ed.* **2001**, *40*, 399.

10.1021/ic7013623 CCC: $37.00
Published on Web 10/31/2007

Table 1. Crystallographic Data for **1**−**4**

	1	**2**	**3**	**4**
empirical formula	$C_{318}H_{306}Cl_{11}Cu_9N_{72}O_{95}S_{14}$	$C_{228}H_{221}Cl_{12}Cu_6N_{48}O_{79}S_5$	$C_{200}H_{168}Cu_6N_{60}O_{64}S_4$	$C_{432}H_{384}Cu_{12}N_{120}O_{120}$
fw	8067.00	5864.47	4945.42	9939.07
wavelength, Å	0.70000	0.70000	0.70000	0.74999
cryst syst	hexagonal	monoclinic	orthorhombic	cubic
space group	$P\bar{3}$	$C2/c$	Ccca	$F4\bar{3}$
unit cell dimens	$a = 67.645(10)$ Å, $\alpha = 90°$ $b = 67.645(10)$ Å, $\beta = 90°$ $c = 21.559(4)$ Å, $\gamma = 120°$	$a = 40.650(8)$ Å, $\alpha = 90°$ $b = 26.670(5)$ Å, $\beta = 110.02(3)°$ $c = 43.877(9)$ Å, $\gamma = 90°$	$a = 26.360(5)$ Å, $\alpha = 90°$ $b = 35.070(7)$ Å, $\beta = 90°$ $c = 38.697(8)$ Å, $\gamma = 90°$	$a = 55.983(7)$ Å, $\alpha = 90°$ $b = 55.983(7)$ Å, $\beta = 90°$ $c = 55.983(7)$ Å, $\gamma = 90°$
V (Å^3)	85 433(24)	44 694(15)	35 773(12)	175 459(35)
Z	6	4	4	8
D_{calcd} (Mg/m^3)	0.941	0.872	0.918	0.753
absn coeff (mm^{-1})	0.491	0.431	0.435	0.336
F(000)	24 900	12 060	10 152	40 992
independent reflns	53 033 [R(int) = 0.1111]	37 213 [R(int) = 0.0573]	16 474 [R(int) = 0.0489]	18 257 [R(int) = 0.0699]
goodness-of-fit on F^2	0.852	0.927	1.020	1.029
final R indices [$I > 2\sigma(I)$]	R1 = 0.1307, wR2 = 0.3274	R1 = 0.0791, wR2 = 0.2012	R1 = 0.0818, wR2 = 0.2454	R1 = 0.0659, wR2 = 0.2001
R indices (all data)	R1 = 0.2092, wR2 = 0.3634	R1 = 0.1167, wR2 = 0.2163	R1 = 0.0990, wR2 = 0.2598	R1 = 0.0790, wR2 = 0.2091
largest diff. peak and hole (e Å^{-3})	0.765 and −0.591	1.340 and −0.615	0.705 and −0.974	2.024 and −0.379 e.Å^{-3}

level of generation of building blocks rather than at the level of framework construction.

Recently, we reported the preparation of octahedral nanocages combining triangular facial ligands with square-planar Pd(II) ions.[7] In this study, we tried to expand the metal ion from a square-planar tetratopic Pd(II) ion to a tetragonally distorted octahedral hexatopic metal ion such as Cu(II) ion. Introduction of hexatopic metal ions at the truncated vertices of the octahedral cage transforms the nanocages as potential SBBs because the axial site of the copper(II) ion directed to the exterior of the nanocages can serve as a connecting node for the formation of MOP-based frameworks.

Experimental Section

Materials. All reagents and solvents for syntheses were purchased from commercial sources and used as received.

Instrumentation. Elemental analyses (C, H, and N) were performed at the Elemental Analysis Laboratory of the Korean Basic Science Institute on a CE Flash EA 1112 series elemental analyzer. Infrared spectra were recorded using ATR in the range 4000−600 cm^{-1} on a BioRad FT-IR spectrometer. NMR spectra were obtained using a Varian-300 spectrometer.

Ligand Synthesis. *N*,*N*′,*N*″-Tris(3-pyridinyl)-1,3,5-benzenetricarboxamide (L**1**) and *N*,*N*′,*N*″-tris(4-pyridinylmethyl)-1,3,5-benzenetricarboxamide (L**2**) were prepared by the reported procedure.[7]

Complex Synthesis. Preparation of $[Cu_6L^1{}_8](ClO_4)_{12}$, 1. A 0.0702 g (0.160 mmol) amount of L**1** was dissolved in 5.0 mL of DMSO, and a 0.0462 g (0.125 mmol) amount of copper(II) perchlorate trihydrate was added to this solution. Layering with 3.5 mL of ethanol to 0.5 mL of the above solution for 3 weeks yielded X-ray-quality blue crystals. The isolated crystals were washed several times with mother liquor and washed with water and freeze-dried for a day. Anal. Calcd for $[Cu_6L^1{}_8](ClO_4)_{12}$·5EtOH ($C_{202}H_{174}N_{48}O_{77}Cl_{12}Cu_6$, fw = 5312.59): C, 45.67; H, 3.30; N, 12.66. Found: C, 45.98; H, 3.61; N, 13.09. IR (ATR, ν/cm^{-1}): 3394(br), 3088(w), 2922(w), 2160(w), 2028(w), 1978(w), 1668(m), 1615(w), 1587(m), 1544(s), 1488(s), 1423(s), 1333(m), 1291(s), 1242(m), 1197(w), 1088(s), 1011(s), 951(m), 933(m), 811(m), 734(w), 697(m), 651(w), 622(w). δ_H (300 MHz, DMSO-d_6 in ppm): 11.91 (bs), 9.04 (bs), 8.72 (bs).

Preparation of $[Cu_6L^2{}_8](ClO_4)_{12}$, 2. A 0.192 g (0.400 mmol) amount of L**2** was dissolved in 15.0 mL of DMSO, and a 0.111 g (0.300 mmol) amount of copper(II) perchlorate trihydrate was added to this solution. Layering with 6.0 mL of ethanol to 1.0 mL of the solution for 3 weeks yielded X-ray-quality blue crystals. The isolated crystals were washed several times with mother liquor and washed with water and freeze-dried for a day. Anal. Calcd for $[Cu_6L^2{}_8](ClO_4)_{12}$·3EtOH·24$H_2O$ ($C_{222}H_{258}N_{48}O_{99}Cl_{12}Cu_6$, fw = 5989.46): C, 44.52; H, 4.34; N, 11.23. Found: C, 44.52; H, 3.97; N, 11.18. IR (ATR, ν/cm^{-1}): 3347(br), 3072(w), 2921(w), 2161(w), 2035(w), 1979(w), 1657(s), 1619(s), 1531(s), 1430(s), 1368(w), 1288(s), 1225(w), 1091(s), 1064(s), 1014(s), 952(m), 932(w), 808(m), 781(w), 702(m), 668(w), 622(m). δ_H (300 MHz, DMSO-d_6 in ppm): 9.30(bs), 8.43(bs).

Preparation of $[Cu_6L^1{}_8](NO_3)_{12}$, 3. A 0.351 g (0.800 mmol) amount of L**1** was dissolved in 15.0 mL of DMSO, and a 0.112 g (0.600 mmol) amount of copper(II) nitrate trihydrate was added to this solution. Layering with 3.0 mL of ethanol to 1.0 mL of the solution for 3 weeks yielded X-ray-quality blue crystals and powdered precipitates. IR and NMR analyses of both types of products turned out to be identical. The isolated crystals were washed several times with mother liquor and dried in air at room temperature. Anal. Calcd for $[Cu_6L^2{}_8](NO_3)_{12}$·10DMSO·33H_2O ($C_{212}H_{270}N_{60}O_{103}S_{10}Cu_6$, fw = 6008.69): C, 42.38; H, 4.53; N, 13.99. Found: C, 42.74; H, 4.15; N, 14.14. IR (ATR, ν/cm^{-1}): 3269(br), 3077(w), 2162(w), 2035(w), 1979(w), 1677(s), 1613(w), 1587(m), 1541(s), 1485(s), 1420(s), 1381(m), 1328(s), 1285(s), 1234(s), 1195(m), 1111(m), 1061(w), 1015(s), 952(m), 918(m), 806(m), 772(w), 726(m), 696(s), 651(w). δ_H (300 MHz, DMSO-d_6 in ppm): 11.84 (bs), 9.01 (bs), 8.71 (bs). *Note: Even though crystal structure analysis suggests that the crystals contain at least 32 DMSO molecules and 8 water molecules as structural solvents per cage* ***3****, the elemental analyses were never consistent with the original contents of the crystals despite several attempts because of the sensitivity of the compound to air. The complexes were found to lose some of the solvent molecules in air. This result is also consistent with the TGA data of framework* ***3*** *(see Figure S2 in the Supporting Information).*

Preparation of $[Cu_6L^2{}_8](NO_3)_{12}$, 4. A 0.058 g (0.12 mmol) amount of L**2** was dissolved in 15.0 mL of DMSO, and a 0.017 g (0.091 mmol) amount of copper(II) nitrate trihydrate was added to this solution. Layering with 3.0 mL of ethanol to 1.0 mL of the

(7) Moon, D.; Kang, S.; Park, J.; Lee, K.; John, R. P.; Won, H.; Seong, G. H.; Kim, Y. S.; Kim, G. H.; Rhee, H.; Lah, M. S. *J. Am. Chem. Soc.* **2006**, *128*, 3530.

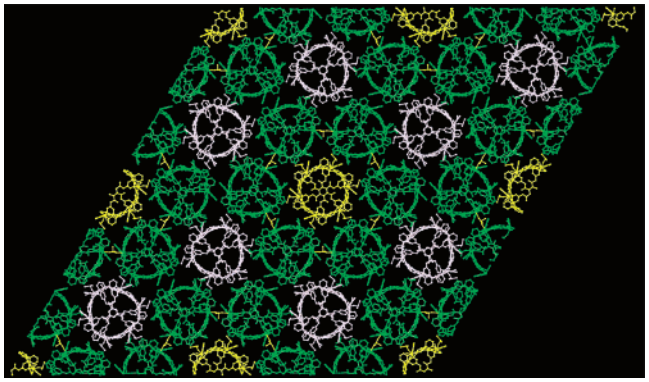

Figure 1. Packing diagram of the crystal structure of $[Cu_6(s\text{-}L^1)_4(a\text{-}L^1)_4]_6[Cu_6(s\text{-}L^1)_6(a\text{-}L^1)_2][Cu_6(s\text{-}L^1)_3(a\text{-}L^1)_5]_2$, **1**, where the green, yellow, and purple nanocages represent the three different types of MOP made of eight C_3-symmetric facial ligands and six Cu(II) ions at the truncated vertices of the octahedron. The perchlorate ions in yellow connect the six green nanocages to form the chair conformational hexameric cluster, and the second type of nanocage in yellow shown at the center and third shown in purple occupy the space between the clusters.

solution for 3 weeks yielded X-ray-quality blue crystals. The isolated crystals were washed several times with mother liquor and washed with water and freeze-dried for a day. Anal. Calcd for $[Cu_6L^2{}_8](NO_3)_{12}\cdot 20DMSO\cdot 52H_2O$ ($C_{256}H_{416}N_{60}O_{132}S_{20}Cu_6$, fw = 7468.92): C, 41.17; H, 5.61; N, 11.25. Found: C, 41.39; H, 5.40; N, 10.80. IR (ATR, ν/cm^{-1}): 3283(br), 3067(w), 2920(w), 2162(w), 2034(w), 1979(w), 1655(s), 1619(s), 1537(s), 1429(s), 1368(s), 1318(s), 1289(s), 1225(m), 1111(w), 1065(m), 1014(s), 952(m), 914(w), 827(w), 808(m), 781(w), 700(m), 668(m). δ_H (300 MHz, DMSO-d_6 in ppm): 9.33 (bs), 8.47 (bs).

X-ray Crystallographic Analysis. The crystals were coated with paratone oil to prevent loss of crystallinity upon exposure to air. The diffraction data were measured at 100 or 86 K with synchrotron radiation (λ = 0.70000 or 0.74999 Å) using a 4AMXW ADSC Quantum-210 detector with a platinum-coated silicon double-crystal monochromator at the Pohang Accelerator Laboratory, Korea. HKL2000 (Ver. 0.98.689)[8] was used for data collection, cell refinement, reduction, and absorption correction. All structures were solved by direct methods and refined by full-matrix least-squares calculations with the SHELXTL-PLUS software package.[9]

1. $[Cu_6(L^1)_8(DMSO)_6][Cu(L^1)_{4/3}(DMSO)][Cu_2(L^1)_{8/3}(DMSO)_2](ClO_4)_2\cdot(DMSO)_{5.5}\cdot(EtOH)_{0.5}\}\cdot 16ClO_4\cdot 26DMSO\cdot 12H_2O$, $C_{370}H_{486}N_{72}O_{161}S_{40}Cl_{18}Cu_9$, M_w = 11 010.78. A crystallographically independent nanocage (octahedral cage complex), one-third of a nanocage in the crystallographic C_3 axis, one-sixth of a nanocage in the crystallographic C_{-3} axis, a ditopic perchlorate ligand between two Cu centers of the adjacent nanocages, a perchlorate anion as monodentate oxygen donor to Cu center, seven additional perchlorates as counter anions, and at least 38 additional noncoordinating structural solvent sites were identified as the asymmetric unit. Refinement converged to final a R1 = 0.2703 ($I > 2\sigma(I)$), wR2 = 0.6251 for all data, GOF = 1.814, max/min residual electron density 1.261/−0.817 e Å.^{3} Structure refinement following modification of the data for electron density of the structural solvent region (42 696.7 Å^3, 50.0%) in the structural model with the SQUEEZE routine in PLATON[10] led to better refinement. Final R1 = 0.1307 ($I > 2\sigma(I)$), wR2 = 0.3634 (all data) for **1**, $\{[Cu_6(L^1)_8(DMSO)_6][Cu(L^1)_{4/3}(DMSO)][Cu_2(L^1)_{8/3}(DMSO)_2](ClO_4)_2\cdot 5.5(DMSO)\cdot 0.5(EtOH)\}\cdot 16(ClO_4)$. A summary of the crystal and intensity data is given in Table 1.

2. $\{[Cu_6(L^2)_8(EtOH)_2(DMSO)_4](ClO_4)_{12}\}\cdot 37DMSO\cdot 6EtOH\cdot 3H_2O$, $C_{312}H_{486}N_{48}O_{123}S_{41}Cl_{12}Cu_6$, M_w = 8998.71. The octahedral cage complex is in a crystallographic 2-fold symmetry axis. Two copper centers have Jahn−Teller elongated octahedral geometries with four

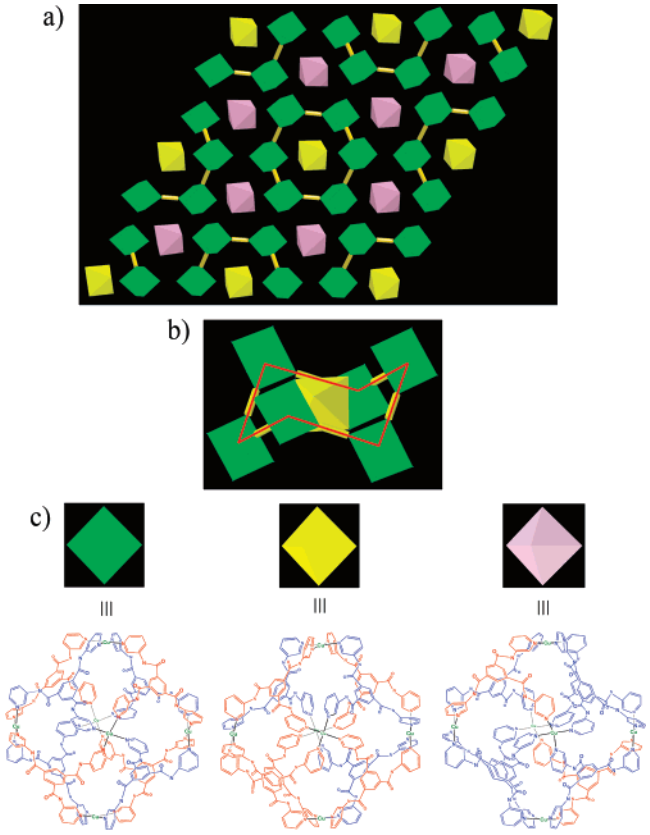

Figure 2. (a) Schematic packing diagram of the crystal structure of $[Cu_6(s\text{-}L^1)_4(a\text{-}L^1)_4]_6[Cu_6(s\text{-}L^1)_6(a\text{-}L^1)_2][Cu_6(s\text{-}L^1)_3(a\text{-}L^1)_5]_2$, **1**, where the green, yellow, and purple octahedra represent the three different types of MOP. The yellow rods connecting the six green octahedra represent the perchlorate ions as ditopic linkers. (b) The chair conformational feature of the hexameric cluster of the first type of nanocages connected via perchlorate ions is highlighted using a red line, and the second type of nanocage is shown in yellow at the center of the cluster. (c) The ligands shown in blue and red represent, respectively, the syn and anti conformations they adopt in the nanocages. In the first type of cage, four ligands are in the syn conformation and the remaining four are in the anti conformation. However, the combination of two conformationally different ligands varies from four/four in the first type of cage to six/two in the second type of cage and three/five in the third type of cage.

Scheme 1. Two Conformations Observed for Ligand L^1 in the Crystal Structure of **1**[a]

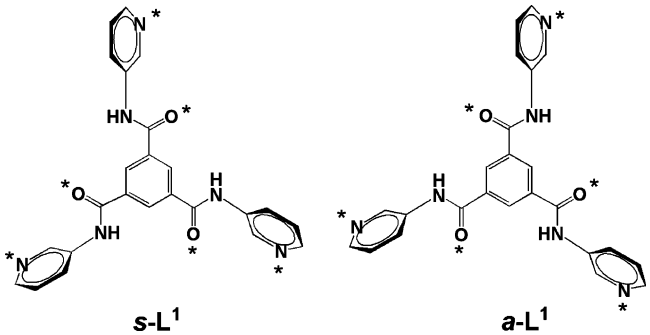

[a] The conformation is defined as *s*-L^1 when the amide oxygen and pyridyl nitrogen are on the same side. The conformation of the ligand is defined as *a*-L^1 when they are opposite.

(8) Otwinowski, Z.; Minor, W. In *Methods in Enzymology*; Carter, C., Jr., Sweet, R. M., Eds.; Academic Press: New York, 1997; Vol. 276, part A, p 307.
(9) Sheldrick, G. M. *SHELXTL-PLUS, Crystal Structure Analysis Package*; Bruker Analytical X-Ray: Madison, WI, 1997.

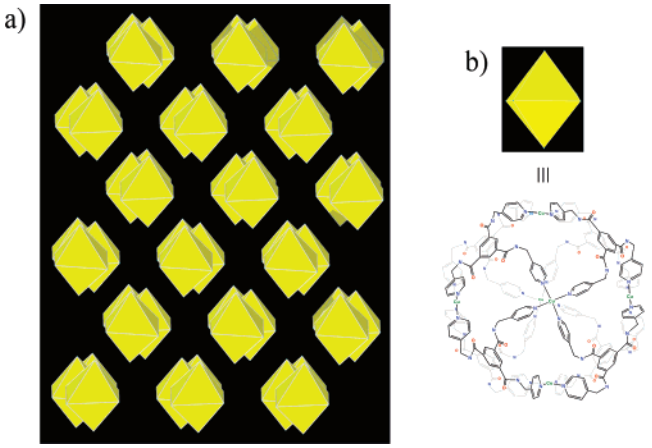

Figure 3. (a) Schematic packing diagram of the crystal structure of $[Cu_6L^2_8]$, **2**, where the yellow octahedron is the schematic presentation of the nanocage. (b) All ligands in the nanocage of the crystal structure of **2** are in the same rotational direction.

pyridyl groups in the equatorial plane, one DMSO near the cavity interior, and the other at the exterior of the cage. One copper center has a square-pyramidal geometry with four pyridyl groups at the basal plane and one ethanol in the cavity interior. At least two perchlorate anions, seven DMSO sites, one ethanol site, and one water in a 2-fold symmetry axis per asymmetric unit were observed in the inner cavity of the nanocages. Seven more DMSO sites and two ethanol sites were observed in the vicinity of the portal areas of the cage. An additional three perchlorate anions, five DMSO molecules, one ethanol, and two water sites were observed at the exterior of the cage. In the crystal structure, a total of 5 perchlorate anions, 21 DMSO molecules including those coordinated to the metal centers, 4 ethanol sites, and 3 water (or partially identified ethanol) sites per asymmetric unit could be identified. Refinement converged to a final R1 = 0.1613 ($I > 2\sigma(I)$), wR2 = 0.4596, GOF = 1.692, max/min residual electron density 2.787/−1.456 e Å^3. Structure refinement following modification of the data for electron density of the structural solvent region (26 578 Å^3, 59.5%) in the structural model with the SQUEEZE routine in PLATON[10] led to better refinement. Final R1 = 0.0791 ($I > 2\sigma(I)$), wR2 = 0.2163 (all data) for **2**, $[Cu_6(L^2)_8(EtOH)_2(DMSO)_4](ClO_4)_{12}$. A summary of the crystal and intensity data is given in Table 1.

3. $[Cu_6(L^1)_8(NO_3)_5(DMSO)_4](NO_3)_7{\cdot}32DMSO{\cdot}8H_2O$, $C_{264}H_{376}N_{60}O_{104}S_{36}Cu_6$, M_w = 7589.67. One-fourth of a nanocage in the crystallographic 222 symmetry site, two disordered ditopic nitrate ligands between two Cu centers of the adjacent nanocages, a nitrate as monodentate anionic ligand at a Cu center, a coordinating DMSO molecule at the remaining Cu center, and at least eight additional noncoordinating DMSO (including one partially identified DMSO site) and two sites corresponding to water molecules were identified as the asymmetric unit. Both copper centers have Jahn−Teller elongated octahedral geometries with four pyridyl groups at the equatorial plane, a DMSO or a nitrate as the fifth ligand near the cavity interior, and a disordered ditopic bridging nitrate as the sixth ligand at the cage exterior. Refinement converged to a final R1 = 0.1297 ($I > 2\sigma(I)$), wR2 = 0.4002 for all data, GOF = 1.632, max/min residual electron density 1.828/−1.165 e Å^3. Structure refinement following modification of the data for electron density of the structural solvent region (19 249 Å^3, 53.8%) in the structural model with the SQUEEZE routine in PLATON[10] led to slightly better refinement. Final R1 = 0.0818 ($I > 2\sigma(I)$), wR2 = 0.2598 (all data) for **3**, $[Cu_6(L^1)_8(NO_3)_5(DMSO)_4](NO_3)_7$. A summary of the crystal and intensity data is given in Table 1.

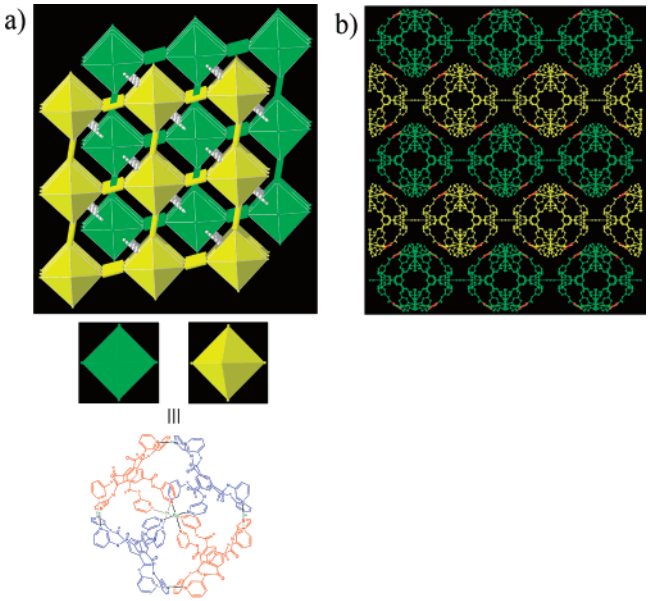

Figure 4. (a) Schematic packing diagram of the crystal structure of $[Cu_6(s\text{-}L^1)_4(a\text{-}L^1)_4]$, **3**. The ditopic nitrate is represented as either a green or a yellow rod, and the $\pi-\pi$ stacking interactions are presented as gray dots. (b) The packing diagram shows the 2-D $\pi-\pi$ stacking interaction. The nitrate appears as if it is a linear triatomic species due to the rotational disordering along the connecting axis. The additional $\pi-\pi$ stacking interaction between the nets occurs through the four facial ligands in the anti conformation in two dimensions, where the benzene moieties of the ligands that participate in the 2-D $\pi-\pi$ stacking interaction are shown in red.

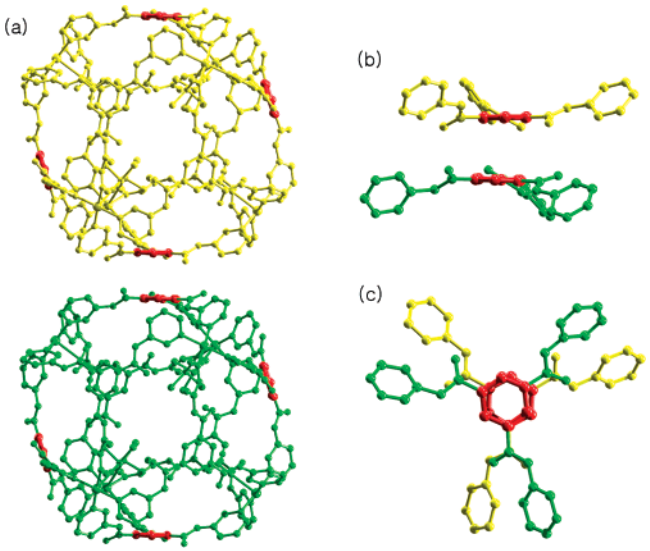

Figure 5. (a) Side view of two nanocages shows a $\pi-\pi$ stacking interaction between the central benzene moieties of the ligands. The $\pi-\pi$ stacking interaction occurs through the four facial ligands in the anti conformation in two dimensions. The benzene moieties of the ligands that participate in the $\pi-\pi$ stacking interaction are shown in red. (b) Side view of the $\pi-\pi$ interacting ligands. (c) Top view of the $\pi-\pi$ interacting ligands.

4. $\{[Cu_6(L^2)_8(NO_3)_3][Cu_6(L^2)_8(NO_3)_9](NO_3)_{12}\}{\cdot}24EtOH{\cdot}120H_2O$, $C_{480}H_{528}N_{120}O_{264}Cu_{12}$, M_w = 12 964.71. Two different types of octahedral cages were identified, and both of them were in a crystallographic tetrahedral symmetry (23 symmetry) site. The cages of the first type were interlinked via a nitrate anion in the crystallographic special position to form a simple cubic net. The sixth coordination site of the metal center on the inside of the cage

(10) Spek, A. L. *Acta Crystallogr., Sect. A* **1990**, *46*, 194.

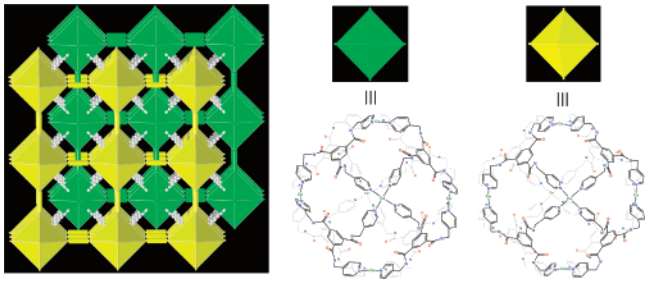

Figure 6. Schematic packing diagram of the crystal structure of $[Cu_6L^2_8]$, **4**, where the yellow and green octahedra represent two different types of nanocages interacting with each other via 3-D $\pi-\pi$ stacking.

is occupied by a partially resolved solvent molecule. The other type of cages was also interlinked to form another independent interpenetrating simple cubic net. In contrast to the first type of cage, the sixth coordination site of the metal center in the interior of the cage is occupied by a partially resolved nitrate anion. Two ethanol molecules and 10 more water sites (or partially resolved ethanol sites) were identified in the difference Fourier map and included in the least-squares refinement. R1 = 0.1187 ($I > 2\sigma(I)$), wR2 = 0.3607 for all data, GOF = 1.029, max/min residual electron density 2.024/−0.379 e Å^3. Structure refinement following modification of the data for electron density of the structural solvent sites and void region (102 840.9 Å^3, 58.6%) in the structural model with the SQUEEZE routine in PLATON[10] led to better refinement. Final R1 = 0.0659 ($I > 2\sigma(I)$), wR2 = 0.2091 (all data) for **4**, $[Cu_6(L^2)_8(NO_3)_3][Cu_6(L^2)_8(NO_3)_9](NO_3)_{12}$. A summary of the crystal and intensity data is given in Table 1. The details of the structural analysis are given in the Supporting Information. CCDC 634515−634518.

Results and Discussion

Layering a DMSO solution of copper(II) ion and the triangular facial ligands, *N*,*N*′,*N*″-tris(3-pyridinyl)-1,3,5-benzenetricarboxamide (L^1) and *N*,*N*′,*N*″-tris(4-pyridinylmethyl)-1,3,5-benzenetricarboxamide (L^2), with ethanol led to either nanosized octahedral MOP, **1** or **2**, or their extended MOFs, **3** or **4**, depending on the anions used.

The combination of L^1 and copper(II) perchlorate led to three slightly different types of nanocages in the ratio 6:1:2 in the crystal structure, namely, $[Cu_6(s\text{-}L^1)_4(a\text{-}L^1)_6][Cu_6(s\text{-}L^1)_6(a\text{-}L^1)_2][Cu_6(s\text{-}L^1)_3(a\text{-}L^1)_5]_2$ **1** (Figures 1 and 2), where the ligand conformations, *s*-L^1 and *a*-L^1, are defined based on the relative orientation of the amide oxygen and the pyridyl nitrogen (Scheme 1). The basic features of these nanocages resemble those of the corresponding Pd(II) analog, $[Pd_6(s\text{-}L^1)_6]$.[7] Eight C_3-symmetric ligands at the octahedral faces are linked via Cu(II) ions at the six truncated octahedral vertices, which led to the truncated octahedral nanocage with 12 portals at the edges. The first type of cage, $[Cu_6(s\text{-}L^1)_4(a\text{-}L^1)_4]$, was connected to form a hexameric cyclic system similar to a cyclohexane ring in its chair conformation using weakly connecting perchlorate anions through the axial site of the copper(II) ion of the cage, where both the cage and the perchlorate anion served as ditopic nodes (Figure 2b). The second type of cage, $[Cu_6(s\text{-}L^1)_6(a\text{-}L^1)_2]$, was located at the center of the hexameric cyclic cluster (Figure 2a and b) and only interacted with other cages via van der Waals interactions. The third type of cage, $[Cu_6(syn\text{-}L^1)_3(anti\text{-}L^1)_5]$, was found between the hexameric cyclic clusters. Even though all cages have pseudo-octahedral symmetry, the strict symmetries of the cages are reduced to lower symmetries due to the various combinational arrangements of the conformationally different facial ligands. The first type cage with $[Cu_6(syn\text{-}L^1)_4(anti\text{-}L^1)_4]$ structure belongs to the *T* point group because all the neighboring conformations of the ligands in the octahedral faces are alternating in two different isomeric forms. In the second type of cage two facial ligands in the anti conformation are in the opposite sides of the octahedral cage, and the remaining six ligands are in the syn conformation. This arrangement of the ligands in the eight faces of the octahedron led to a D_3-symmetric cage. The symmetry of the third type of cage is further reduced to the C_3 point group because one syn conformational ligand of the first type of cage is converted to an anti conformational ligand to form the $[Cu_6(syn\text{-}L^1)_3(anti\text{-}L^1)_5]$ structure.

When L^2 was combined with copper(II) perchlorate, only one type of nanocage, $[Cu_6(L^2)_8]$, was found in the crystal structure, **2** (Figure 3). The nanocage is in the crystallographic 2-fold symmetry axis. Unlike L^1, L^2 does not show any conformational isomerism because of the para positioning of the pyridyl nitrogen. Even though at least 5 perchlorate anions in addition to 21 DMSO molecules, 4 ethanol sites, and 3 water (or partially identified ethanol or DMSO) sites per asymmetric unit could be identified at the inner cavity and exterior of the cage and around the portal area, none of the perchlorate ions is involved in the linkage between the nanocages or ligated to the copper(II) centers.

To produce connectivity between MOP for the preparation of extended frameworks, we replaced the anion of the copper salt from the poor linking ability perchlorate to the better linking nitrate. Both ligands, L^1 and L^2, when treated separately with copper(II) nitrate give nanocages that are linked by nitrate ions as ditopic nodes. The combination of L^1 and copper(II) nitrate gives the 2-fold interpenetrating augmented primitive cubic network, **3** of a nanocage, where the nanocages serve as SBBs of octahedral hexatopic nodes and nitrates as ditopic nodes (Figure 4). The ligands of the cage in framework **3** are in two different conformations, *s*-L^1 and *a*-L^1, that form the $[Cu_6(s\text{-}L^1)_4(a\text{-}L^1)_4]$ cage structure, as in the first type of cage of crystal structure **1**. However, the symmetry of this cage, D_2 point group, is different from that of the cage in crystal structure **1**, *T* point group. Four alternate edge and corner-sharing facial ligands are in the same anti conformation and the remaining four ligands are in the syn conformation. The facial ligands in the syn conformations have an inward curvature providing a concave cage surface, while the ligands in the anti conformations have an outward curvature providing a convex surface. The convex surfaced ligand units in one network are involved in $\pi-\pi$ stacking interactions using their central benzene moieties with the same convex surfaced ligand units in the other interpenetrating network (Figure 5), which leads to two-dimensional propagation of the $\pi-\pi$ stacking interaction (Figure 4b).

Although the combination of L^2 and copper(II) nitrate forms 2-fold interpenetrating augmented primitive cubic

Scheme 2. Conformational Isomerism Observed for the Arrangements of Ligand L^2 in the Nanocages of the Crystal Structures of **2** and **4**[a]

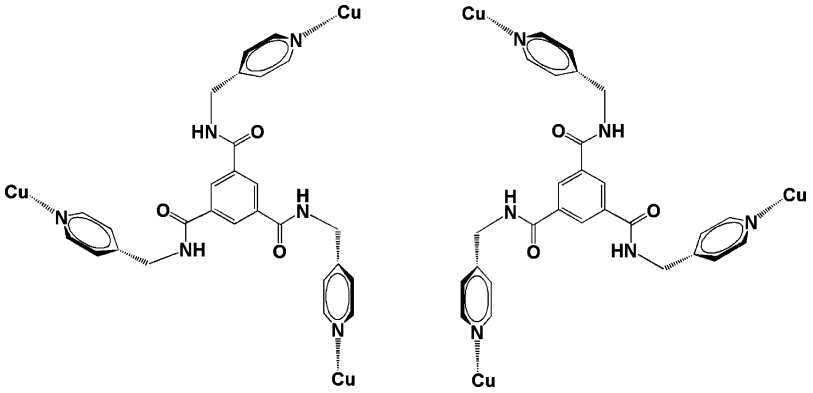

[a] The ligands in the faces of the octahedral cage can have two different conformations depending on the rotational arrangement of the amide group vs the central benzene moiety in either the right- or the left-handed rotational sense.

framework **4**, the nanocages are different from that of framework **3**. Even though only one type of ligand conformation is possible, the arrangement of the C_3-symmetric ligands in the eight faces of the octahedral cage can lead to another level of conformational isomerism, as shown in Figure 6. In the first type of cage $[Cu_6(L^2)_8]$ of net **4** all the facial ligands are in the same rotational direction as in the cage of crystal structure **2**, while all the ligands in the other type of cage are alternating in their rotational direction (Scheme 2). All the ligands in the cages of framework **4** have an outward curvature and are involved in a $\pi-\pi$ stacking interaction as in framework **3**, while the stacking interactions propagate in three dimensions (Figure 6). The solvent cavity percentage of framework **4**, 59%, is slightly larger than that of framework **3**, 54%.[8] The increase of the solvent cavity percentage in framework **4** is mainly due to the increase in the cavity volume of the nanocage in framework **4** over that in framework **3**.

Conclusions

Use of C_3-symmetric ligands as triangular facial ligands and a tetragonally distorted octahedral metal ion such as Cu(II) ion for a vertex node can generate either truncated octahedral nanocages of pseudo-*O* symmetry or MOFs based on the nanocages as SBBs depending on the nature of the anions employed either as counteranion or ditopic linker anion. Replacement of the metal ion from the tetratopic square-planar Pd(II) ion to the potential hexatopic Cu(II) ion yields either the unconnected discrete nanocages or their 3-D networks depending on the linking ability of the anions used. The perchlorate ion with poor linking capability resulted in unconnected nanosized cages, while the nitrate anion with better linking ability led to 2-fold interpenetrating MOFs having an augmented primitive 3-D cubic network topology, where the nanocages served as SBBs of the frameworks. The MOFs retain the cavities that inherently belong to the MOP despite the interpenetration. In addition, the size of the cavities can be tuned based on the cavity size of the building blocks.

Acknowledgment. This work was supported by KRF (KRF-2005-070-C00068), KOSEF (R01-2007-000-10167-0), and CBMH. The authors also acknowledge PAL for beam line use (2006-3041-23).

Supporting Information Available: X-ray crystallographic file in CIF format for the structure determination. This material is available free of charge via the Internet at http://pubs.acs.org.

IC7013623